Electrical and microstructural properties of microwave sintered SnO_2-based varistors

(Propriedades elétricas e microestruturais de varistores à base de SnO_2 sinterizados por microondas)

P. S. Furtado[1], M. M. Oliveira[1], J. S. Vasconcelos[1], J. H. G. Rangel[1], E. Longo[2], V. C de Sousa[3]
[1]IFMA-DAQ- PPGEM, Av. Getúlio Vargas 04, S. Luís, MA 65025-001
[2]CMDMC, LIEC, Instituto de Química, UNESP, C.P. 355, Araraquara, SP 14801-907
[3]DEMAT, Universidade Federal do Rio Grande do Sul - UFRGS, Campus do Vale, Av. Bento Gonçalves 9500, Setor 4, P. 74, 1° andar, S. 213, Porto Alegre, RS 91501-970
periclesft@ifma.edu.br, marcelo@ifma.edu.br, jomar@ifma.edu.br, hiltonrangel@ifma.edu.br, elson@iq.unesp.br, vania.sousa@ufrgs.br

Abstract

An investigation was made of the microstructural and electrical properties of SnO_2-based varistors microwave sintered at 1200 ºC, applying a heating rate of 120 ºC/min and treatment times of 10, 20, 30, 40, 50 and 60 min. The system used in this study was (98.95-X)%SnO_2.1.0%CoO.0.05%Cr_2O_3.X%Ta_2O_5, where X corresponds to 0.05 and 0.065 mol%. Sintering was carried out in a domestic microwave oven (2.45 GHz) fitted for lab use. Silicon carbide was placed in a refractory vessel to form a heating chamber surrounding the sample holder. The pellets were examined by scanning electron microscopy, X-ray diffractometry, direct current measurements and impedance spectroscopy. The parameters of density, medium grain size, coefficient of nonlinearity, breakdown electrical field, leakage current, and height and width of the potential barrier were analyzed.
Keywords: microwave sintering, electrical properties, SnO_2, varistors.

Resumo

Foi feito um estudo das propriedades microestruturais e elétricas de varistores à base de SnO_2, sinterizados por microondas a 1200 ºC, com uma taxa de aquecimento de 120 ºC/min e tempos de tratamento de 10, 20, 30, 40, 50 e 60 min. O sistema utilizado neste estudo foi de (98,95-X)%SnO_2.1,0%CoO.0,05%Cr_2O_3.X%Ta_2O_5, onde X corresponde a 0,05 e 0,065 mol%. A sinterização foi feita em um forno de microondas doméstico (2,45 GHz), equipado para uso em laboratório. Carbeto de silício foi colocado em um recipiente refratário para formar uma câmara de aquecimento em torno do suporte da amostra. As amostras foram analisadas por microscopia eletrônica de varredura, difração de raios X, medições de corrente dc e espectroscopia de impedância. Os seguintes parâmetros foram analisados: densidade, tamanho médio de grão, coeficiente de não-linearidade, campo de rigidez dielétrica, corrente de fuga, e altura e largura da barreira de potencial.
***Palavras-chave**: sinterização por microondas, propriedades elétricas, SnO_2, varistores.*

INTRODUCTION

The addition of different dopants to varistor systems, especially SnO_2-based, has strongly influenced the nonlinear properties which are responsible for the varistor behavior of these ceramic devices, altering defects in the conduction barrier and in their working voltage, which is associated to the breakdown electrical field [1-4]. A review of the effect of donor metals on the electrical and microstructural properties of SnO_2-based ceramic varistors was done and it was found that some of these oxides, such as Cr_2O_3 and La_2O_3, significantly improve the electrical properties of varistors while others, such as Bi_2O_3 and Er_2O_3, for instance, do not have this effect [5]. The evolution of the varistor performance has also been attributed to oxygen species produced by the reaction with these dopants. Other ways to improve these properties is by working with process parameters, one of which is the treatment time at sintering temperature. One of the sintering techniques that have been studied is microwave-assisted sintering. This technique involves rapid heating of the sample, followed by sintering at a high temperature in a short period of time, and may culminate in products with higher density and smaller grain size than those obtained by conventional sintering [6]. An important aspect of microwave heating is the direct absorption of energy by the material to be heated, unlike heating by convection, whereby energy is transferred slowly from the reaction vessel to the sample. Thus, microwave heating is selective and will depend mainly on the dielectric constant and the relaxation frequency of the material [7].

Microwave sintering of ZnO-based electronic ceramics has been investigated and shown satisfactory results when compared to the conventional method, with high heating rates, lower sintering temperatures, shorter times, and hence, lower energy consumption [8-10].

The objective of this work was to study the effect of treatment time at the sintering threshold on the electrical and microstructural properties of the SnO_2.CoO.Cr_2O_3.Ta_2O_5 system.

EXPERIMENTAL DETAILS

The materials were prepared in several processing stages, from the mixing of powders to their compaction to obtain green pellets. The oxides used were: SnO_2 (Merck), CoO (Aldrich), Cr_2O_3 (Aldrich) and Ta_2O_5 (Mamoré), all in the form of powder of analytical grade. The compositions used were (98.90)%SnO_2.1.0%CoO.0.05%Cr_2O_3.0.05%Ta_2O_5 and (98.885)%SnO_2.1.0%CoO.0.05%Cr_2O_3.0.065%Ta_2O_5, referred to hereafter as SCCrTa5 and SCCrTa6, respectively.

The ceramic powders were mixed, ground and homogeneized by wet ball milling with isopropyl alcohol P.A. in polypropylene jars for 6 h. The powders were then oven-dried at 100 ºC for 4 h. They were deagglomerated by hand and granulometrically classified in a 100 mesh sieve (150 μm). The powders were compacted under uniaxial and isostatic pressure (150 MPa) to increase their green density. Microwave sintering was carried out in a Sanyo domestic microwave oven with 1300 W power and a standard frequency of 2.45 GHz, adapted for lab use. The pellets were placed in a refractory vessel containing, in the central portion, silicon carbide which acts as a susceptor and thus as heat source. The use of a susceptor is necessary due to the transparent behavior of tin oxide at room temperature at 2.45 GHz. The program consisted of a heating rate of 120 ºC/min,dwelling of 1200 ºC, treatment time of 10, 20, 30, 40, 50 and 60 min, and cooling to room temperature. The nomenclature used in the microwave sintering process was based on the following criteria: the first algorism refers to the percent of Ta_2O_5, as indicated in Table I, and the second corresponds to the treatment time in the oven, where 1=10 min, 2=20 min, 3=30 min, 4=40 min, 5=50 min and 6=60 min. This means that for the SCCrTa56 system, number 5 indicates the composition, which in this case is 0.05% of Ta_2O_5 sintered for 60 min, while for SCCrTa61, number 6 indicates the composition 0.065% of Ta_2O_5 sintered for 10 min.

The geometric method was employed to determine the densities of green and sintered pellets. The X-ray diffractograms were obtained with a high resolution X-ray diffractometer (Rigaku Dmax/2500PC), using Cukα radiation and 2θ varying from 25° to 75°. Micrographs were recorded on a field emission scanning electron microscope (FEG-SEM, Carl Zeiss LEO 1550). The samples were sandpapered, polished and thermally etched TS-50 ºC, where TS is the temperature at which the samples were sintered [9, 11]. The mean grain diameters were determined by the method of intercepts. A stabilized pulse voltage supply (Keythley 237) was used to monitor the characteristic current density curve as a function of the electrical field (J x E) at room temperature, from which the coefficient of nonlinearity α, the breakdown electrical field E_r, and the leakage current (I_f) were obtained.

The sample surfaces were sandpapered and polished to render them flat and parallel, after which they were coated with silver paint, placed in a muffle furnace and treated at 400 ºC for 15 min to fix the electrodes. The electric field E and current density J were determined from the measurement of the electrical current I generated when subjected to an electric voltage V, using equations A and B.

$$E = V / d \quad (A)$$

$$J = I / A \quad (B)$$

where d is the thickness of the sample (cm) and A the area of the electrode coated on the surface of the sample (cm^2). The values of the coefficients of nonlinearity α were obtained by means of linear regression of the *Log J x Log E* curve and from J = 1 $mA.cm^{-2}$, and the breakdown electrical field E_r was determined at this point E *1mA.cm*$^{-2}$. The leakage current I_f was determined, comparatively, as the value of the voltage corresponding to 70% of the breakdown electrical field [11-13]. The effective barrier voltage was obtained by equation (C).

$$V_b = E_r \bar{d} \quad (C)$$

where $\bar{d}$ is the mean grain diameter. The accuracy of these calculations is not of course very high, since in reality the average grain diameter is a statistical parameters [14, 15]. Impedance was measured with a Solartron 1260 impedance analyzer, at frequencies varying from 1 Hz to 1 MHz, with an amplitude of 1 V and, by the second method, with a compound signal (dc andac), with V_{DC} varying from 0 to 38 V and the ac component set at a frequency of 1 MHz to obtain the grain-boundary capacitance, all at room temperature.

RESULTS AND DISCUSSION

Pure SnO_2 presents low density, but when doped with CoO, the diffusion mechanism increases, promoting larger densification. When microwave sintered, the same compositions converged toward larger densification (about 99% of the theoretical density) for 60 min in the oven, since longer sintering times promote grain growth and tend to eliminate pores, as shown in Table I.

The X-ray diffraction analyses indicated that no other phases were formed besides SnO_2 cassiterite, according to JCPDS 41-1445 file, Fig. 1. The absence of secondary phase is likely due to the small dopant contents in SnO_2. However, as the treatment time in the oven increased from 10 to 50 min, the basal planes became well-defined.

Fig. 2 shows the SEM micrographs of the microwave

Table I - Density of the microwave sintered compositions.
[Tabela I - Densidade das composições sinterizadas por microondas.]

Composition	Treatment time (min)	Density ($g.cm^{-3}$)	Relative density (%)
SCCrTa51	10	6.69	96.31
SCCrTa52	20	6.80	97.81
SCCrTa53	30	6.84	98.49
SCCrTa54	40	6.87	98.92
SCCrTa55	50	6.87	98.85
SCCrTa56	60	6.92	99.50
SCCrTa61	10	6.69	96.26
SCCrTa62	20	6.74	97.00
SCCrTa63	30	6.85	98.54
SCCrTa64	40	6.85	98.60
SCCrTa65	50	6.87	98.89
SCCrTa66	60	6.93	99.76

sintered compositions, while Fig. 3 depicts the variation in mean grain size as a function of treatment time. These micrographs do not show the formation of other phases, which is consistent with the XRD results. As expected, the mean grain sizes calculated for the microwave sintered compositions were smaller than those of sintered conventionally compositions [16], since higher heating rates and shorter treatment times in the oven promote this effect [17]. All the compositions showed slight grain growth with the variation of treatment time up to 50 min, above which the SCCrTa56 and SCCrTa66 compositions showed a reduction at 60 min (Fig. 3), which may be ascribed to the increase in the amount of dopant.

Fig. 4 depicts the *J x E* curves of the microwave sintered compositions. Table II lists the parameters obtained by direct current measurements: coefficient of nonlinearity, α, breakdown electric field, E_r, mean grain diameter, $\overline{d}$, barrier voltage, v_b and leakage current, I_f, of the microwave sintered compositions. The dc measurements of the microwave sintered compositions (Fig. 4) demonstrated that the SCCrTa5 samples presented better performance with respect to α and high E_r values of up to 27.450 $V.cm^{-1}$ in the SCCrTa53 samples. Varistors with good performance should show high values of v_b and low values of I_f. Barrier voltages v_b are associated with the height of the effective potential barrier, while high leakage currents I_f promote greater production of heat by the Joule effect, causing deterioration of the nonohmic properties of varistors [13]. As can be seen in Table II, the SCCrTa5 (0.05% Ta_2O_5) composition presented the best results at treatment times of 30, 40, 50 and 60 min (indicated, respectively, by SCCrTa53, SCCrta54, SCCrTa55 and SCCrTa56).

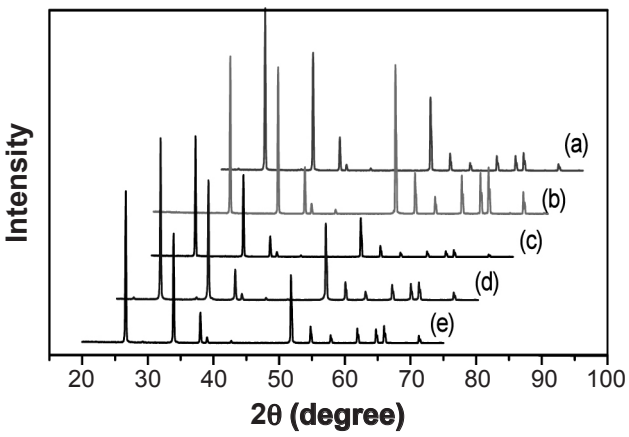

Figure 1: X-ray diffraction patterns of the varistor systems: a) SCCrTa51; b) SCCrTa52; c) SCCrTa53; d) SCCrTa61 and e) SCCrTa62.
[Figura 1: Difratogramas dos sistemas varistores: a) SCCrTa51; b) SCCrTa52; c) SCCrTa53; d) SCCrTa61 e e) SCCrTa62.]

The conductivity of oxide-based ceramics depends on the characteristics of the samples, such as chemical composition, purity, microstructural homogeneity, pore volume and distribution, and grain size. The total resistivity of polycrystalline materials is the sum of the intragranular and intergranular contribution. Direct current measurements provide only the value of total conductivity, but give no information about the grain and grain boundary contribution to the conductivity or about the effect of the electrodes. To overcome these limitations, impedance measurements are taken with alternating current, represented on the complex plane. Fig. 5 shows Nyquist plots of the compositions.

All compositions displayed behavior similar to those reported [18]. Fig. 6 depicts a traditional model of an equivalent circuit for varistors and the circuit parameter values obtained using Zview® software.

As can be observed the Nyquist plots of some microwave sintered compositions do not form a complete semicircle (flattened), showing, instead a decreasing straight line in the Bode plots (Fig. 7). These samples presented very high impedances in the frequency range used in the measurements (1 Hz to 1 MHz), associated with the smaller grain sizes (between 0.73 and 1.60 μm). The grain resistance and brain boundary values obtained for the microwave sintered samples were high (~10^6 and 10^9 Ω, respectively).

The Rs resistances presented maximum values in the order of 10^2, while the grain and grain boundary resistances presented minimum values in the order of 10^4. Therefore, Rs could be considered as electrode resistance and not strongly influence the circuit parameters adjusted for the model in Fig. 6 or for the model without Rs resistance, as reported in the literature [19]. Other more complex models, which incorporate the influence of charge densities in the grains associated with the thickness of the intergranular layer, have been reported [20].

Fig. 8 shows the capacitance behavior of the microwave

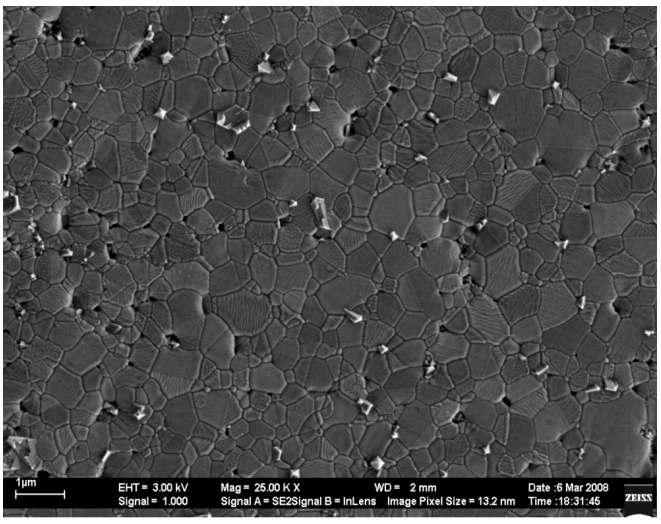

SCCrTa51

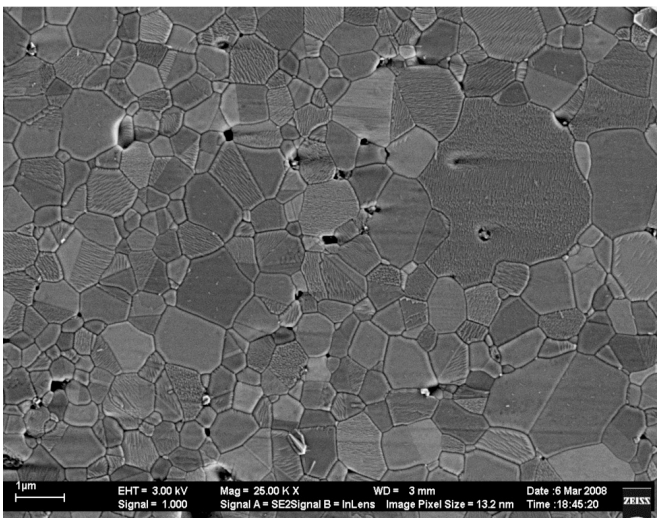

SCCrTa51

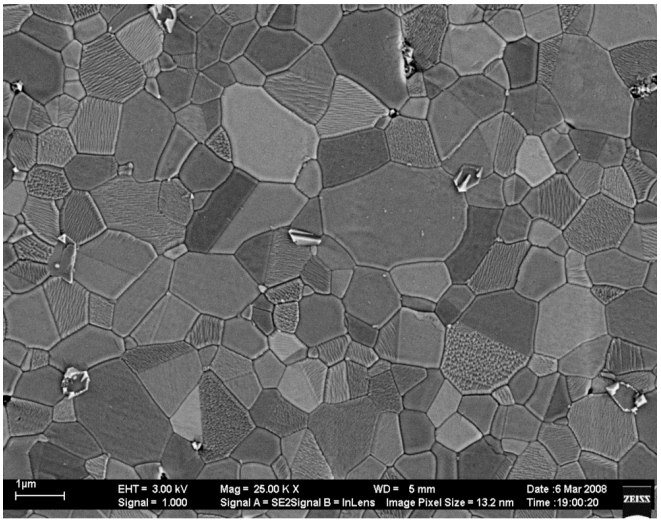

SCCrTa55

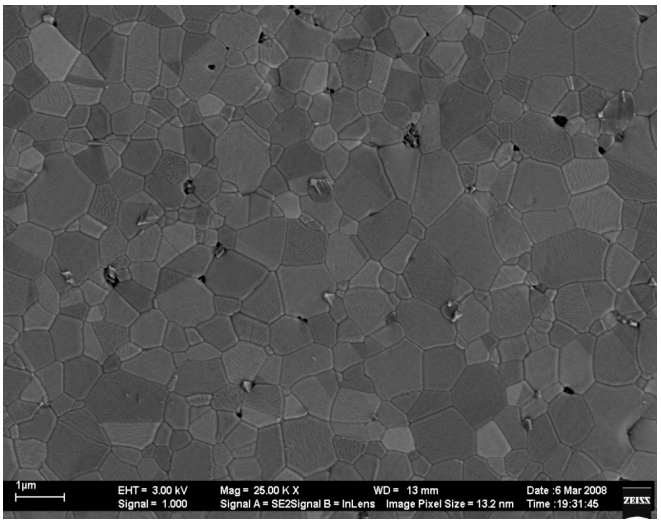

SCCrTa61

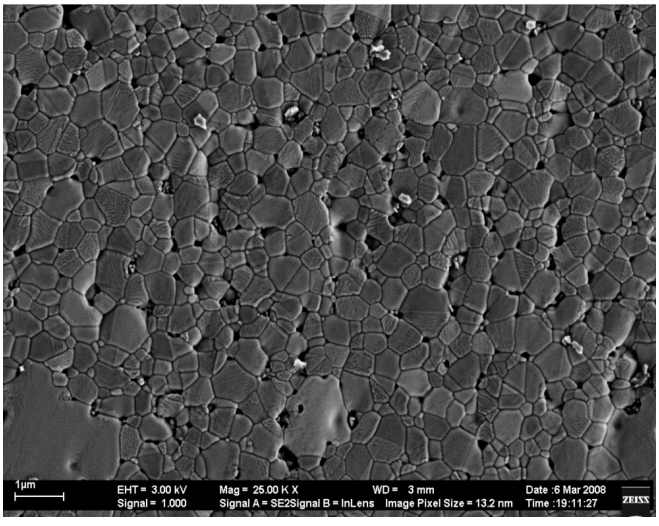

SCCrTa63

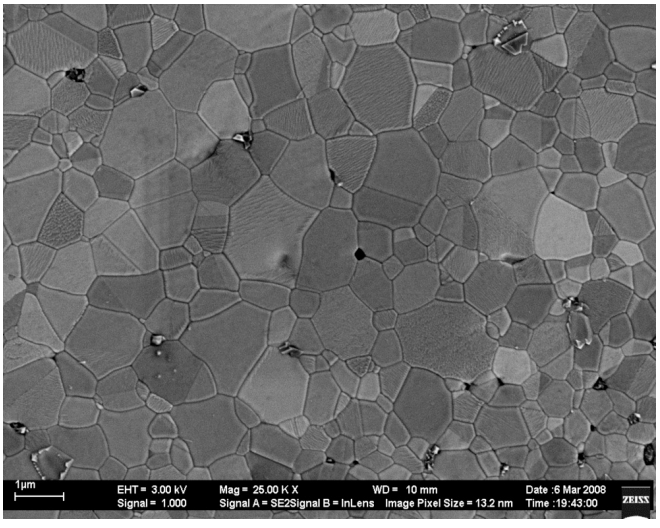

SCCrTa65

Figure 2: SEM micrographs of the compositions microwave sintered for 10, 30 and 50 min.
[Figura 2: Micrografias obtidas por MEV das composições sinterizadas por microondas por 10, 30 e 50 min.]

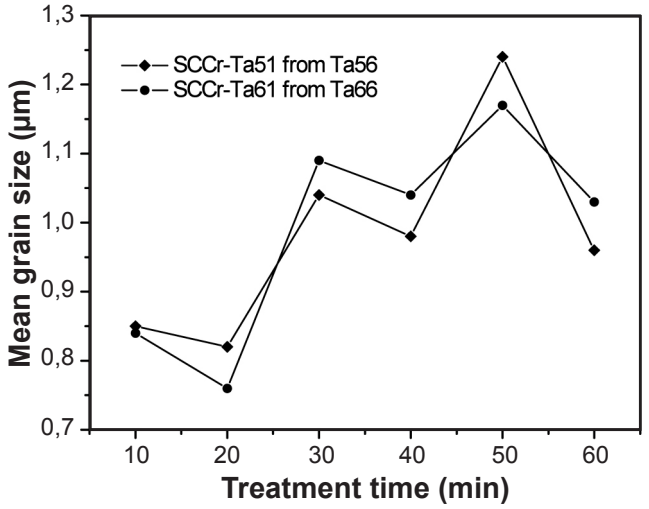

Figure 3: Variation of mean grain size of microwave sintered compositions as a function of treatment time.
[Figura 3: Variação do diâmetro médio de grão das composições sinterizadas por microondas em função do tempo de sinterização.]

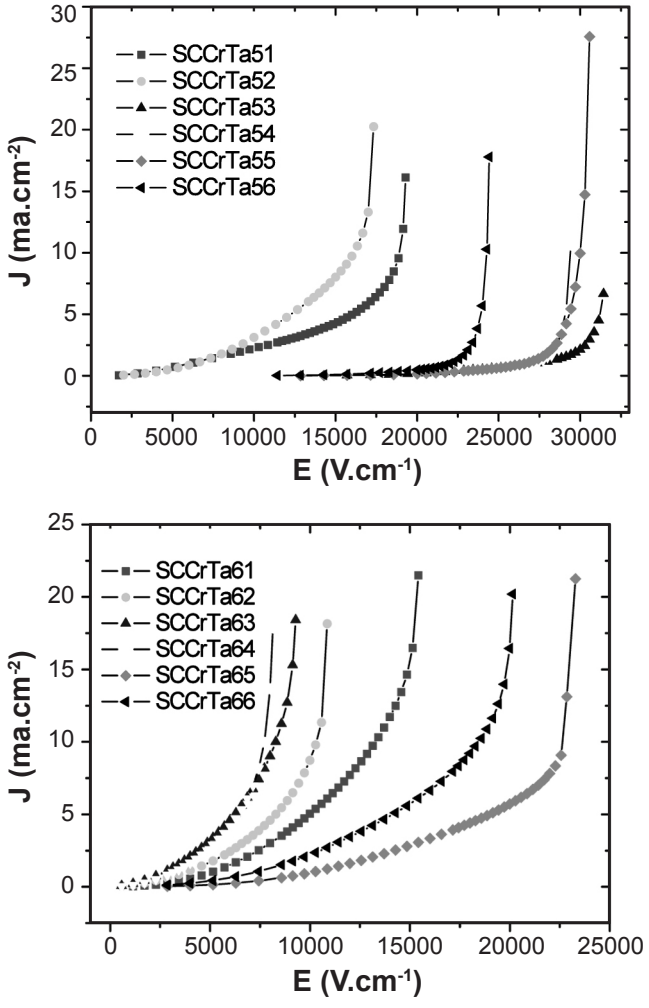

Figure 4: The J - E curves of the microwave sintered compositions.
[Figura 4: Curvas de J - E para as composições sinterizadas por microondas.]

Table II - Parameters obtained by dc measurements of the microwave sintered compositions.
[Tabela II - Parâmetros obtidos por meio de medidas dc das composições sinterizadas por microondas.]

Compositions	α	E_r (V.cm^{-1})	$\bar{d}$ (μm)	v_b (V/b)	I_f (μA)
SCCrTa51	1.8	6193	0.85	0.53	178
SCCrTa52	2.5	6450	0.82	0.53	148
SCCrTa53	13	27450	1.04	2.85	42
SCCrTa54	38	27350	0.98	2.68	45
SCCrTa55	23	26600	1.24	3.30	51
SCCrTa56	28	22100	0.96	2.12	48
SCCrTa61	2.4	4900	0.84	0.41	154
SCCrTa62	2.3	3800	0.76	0.29	184
SCCrTa63	2.1	2750	1.09	0.30	183
SCCrTa64	2.4	3050	1.04	0.32	178
SCCrTa65	2.7	10000	1.17	1.17	125
SCCrTa66	2.4	7360	1.03	0.76	158

can also check using Table II that the processing time was not sufficient to obtain and varistor properties with increasing the amount of tantalum, there was a degradation of varistor properties.

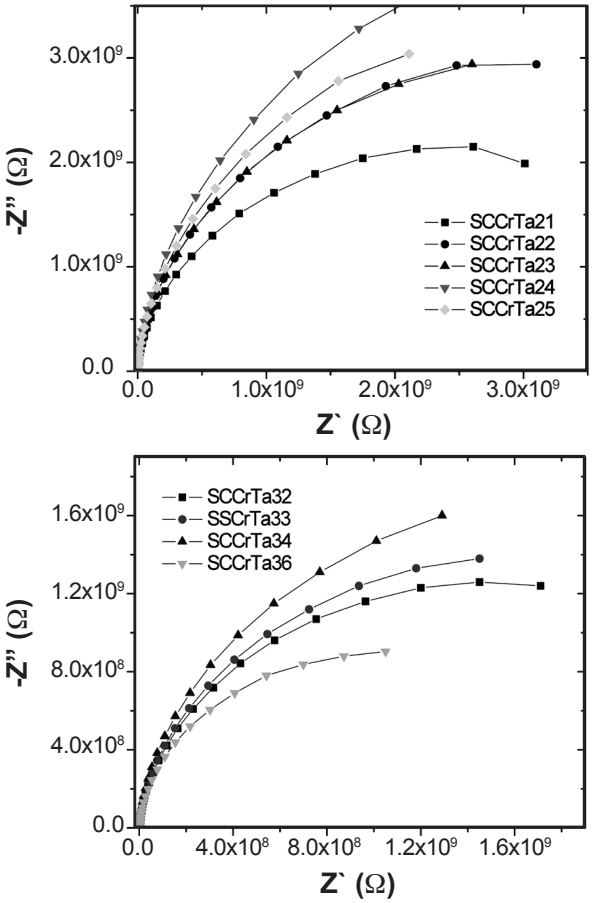

Figure 5: Nyquist plots of the microwave sintered compositions.
[Figura 5: Gráfico de Nyquist das composições sinterizadas por microondas.]

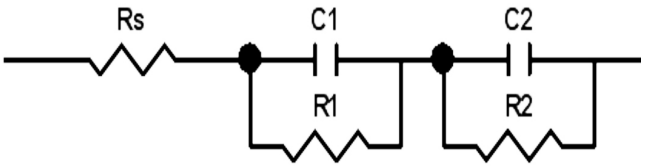

Figure 6: Equivalent circuit for the microwave sintered compositions.
[Figura 6: Circuito equivalente para as composições sinterizadas por microondas.]

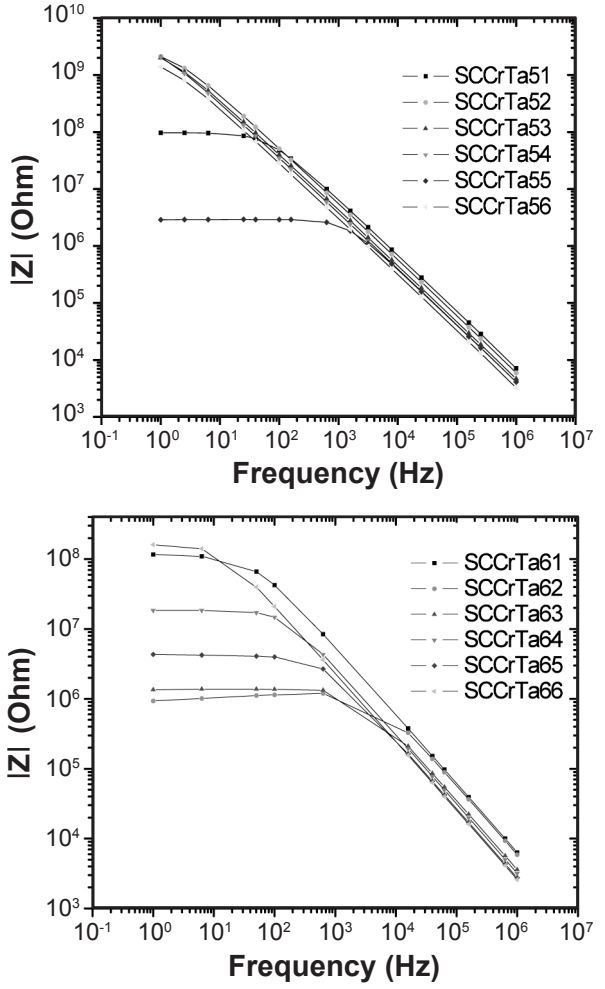

Figure 7: Bode plots of the microwave sintered compositions.
[Figura 7: Gráfico de Bode das composições sinterizadas por microondas.]

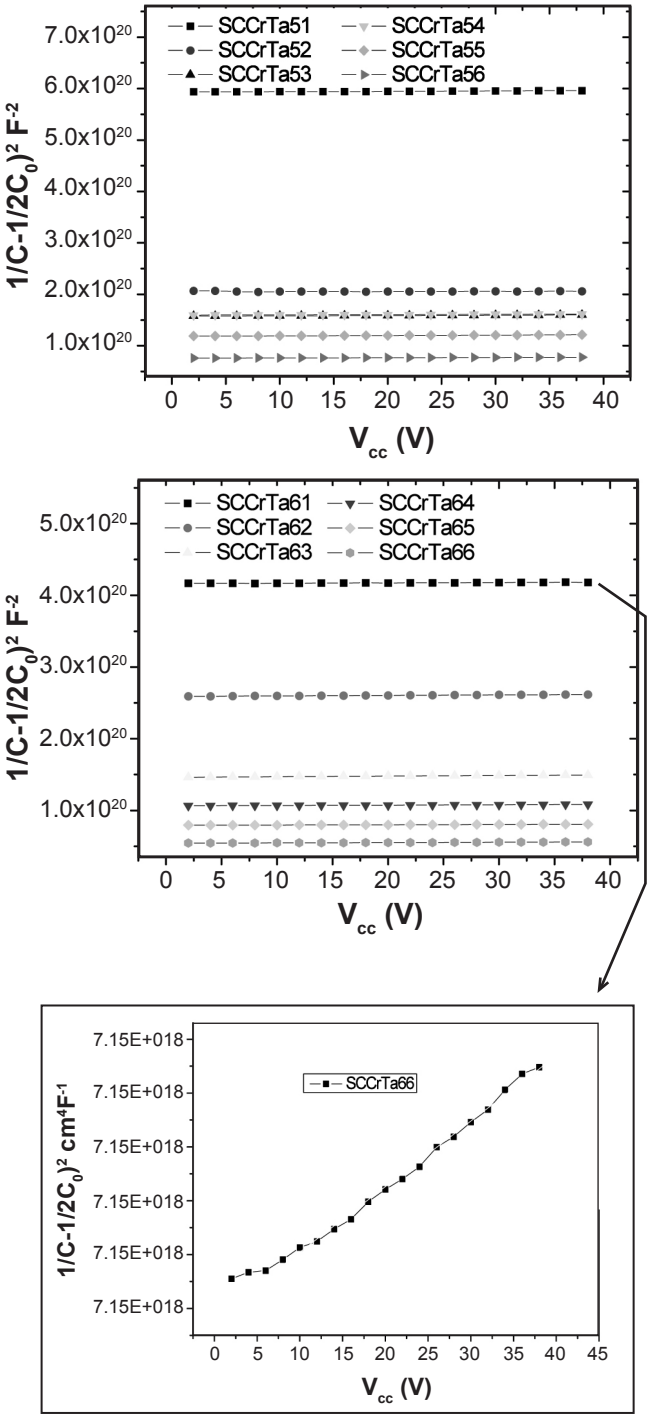

Figure 8: C vs. V plots of the microwave sintered compositions.
[Figura 8: Gráfico de C versus V das composições sinterizadas por microondas.]

sintered compositions as a function of voltage (C vs. V curve), obtained by impedance spectroscopy at room temperature. All these *C vs. V* curves displayed a Mott-Schottky behavior, indicating the existence of a Schottky-type potential barrier (back-to-back barrier), since the capacitances $(C_{BL})^{-2}$ increased with the increase in the voltage composed of a variable signal in direct current (bias) and an alternating signal at a fixed frequency of 1 MHz. This behavior was observed in both ZnO-based and SnO_2-based varistors, which, despite their distinct microstructural nature, share the same physical nature of the potential barrier, which is related to the presence of oxygen species at the grain boundary [21-24]. Table III lists the parameters obtained from these graphs.

Some values of ϕ_b, N_d, N_{IS} and δ do not follow a logical sequence, since it was expected that increasing the nonlinear coefficient (α) would cause the height of the potential barrier to increase. This behavior can be attributed to the number of effective barriers of the varistor, i.e., the larger the number

Table III - ϕ_b , N_d , N_{IS} , and δ values for a back-to-back Schottky-type potential barrier of SCCrTa varistor systems. These calculations take into consideration the average number of grains between electrodes.
[Tabela III - Valores de ϕ_b , N_d , N_{IS} , e δ para barreira de potencial tipo Schottky back-to-back dos sistemas varistores SCCrTa. Esses cálculos levaram em consideração o número médio de grãos entre os eletrodos.]

Compositions	α	ϕ_b (V)	N_dx10^{23} (m^{-3})	N_{IS}x10^{16} (m^{-2})	δ (ηm)
SCCrTa51	1.8	0.22	5.25	3.30	9.66
SCCrTa52	2.5	0.35	4.70	8.10	9.56
SCCrTa53	13	2.24	3.61	7.03	9.73
SCCrTa54	38	3.03	4.68	7.91	8.45
SCCrTa55	23	2.74	3.39	5.94	8.77
SCCrTa56	28	2.97	4.17	5.13	6.15
SCCrTa61	2.4	0.21	6.61	4.60	8.02
SCCrTa62	2.3	0.43	5.12	8.17	7.98
SCCrTa63	2.1	0.58	3.31	5.35	8.08
SCCrTa64	2.4	0.81	5.69	7.15	6.28
SCCrTa65	2.7	0.87	6.04	7.41	6.13
SCCrTa66	2.4	0.29	5.00	5.31	0.05

of barriers the higher the varistor response.

CONCLUSIONS

SnO_2-based varistors processed by microwave radiation presented coefficients of nonlinearity associated with a new sintering kinetics; larger breakdown electric fields associated with the microstructure of smaller grain sizes; and lower leakage currents associated with high potential barriers. Not all the systems showed a good correlation among the values of ϕ_b, N_d, N_{IS} and ω, but microwave sintering proved effective in obtaining electronic ceramics in short sintering times and satisfactory electrical properties.

ACKNOWLEDGMENTS

The authors acknowledge Eletronorte, CAPES, FAPEMA and CNPq for the financial support of this work, LIEC-UFSCar for the FEG-SEM and X-ray measurements, and Prof. Dr. C. William of UFMA for the impedance measurements and discussion thereof.

REFERENCES

[1] T. K. Gupta, A. C. Miler, J. Mater. Res. **3**, 4 (1988) 745.
[2] T. Miyosh, K. Maede, K. Takahashi, T. Yamazaki, *Advances in Ceramics*, Am. Ceram. Soc., Columbus, OH, EUA (1981) 309.
[3] S. R. Dhage, V. Ravi, S. K. Date, Bull. Mater. Sci. **27**, 1 (2004) 43.
[4] S. A. Pianaro, P. R. Bueno, P. Olivi, E. Longo, J. A. Varela, J. Mater. Sci. Lett. **16**, 8 (1997) 634.
[5] M. M. Oliveira, J. H. G. Range1, V. C. de Sousa, E. Longo, R. N. R. Filho, Cerâmica **54**, 331 (2008) 296.
[6] G. J. Pereira, D. Gouvêa, Cerâmica **49**, 310 (2003) 116.
[7] F. Rosini, C. C. Nascentes, J. A. Nobrega, Quím. Nova **27**, 6 (2004) 1012.
[8] I. N. Lin, W. C. Lee, K. C. Liu, H. F. Cheng, M. W. Wu, J. Eur. Ceram. Soc. **21** (2001) 2085.
[9] L. Cong, X. Zheng, P. Hu, S. Dan-feng, J. Am. Ceram. Soc. **90**, 9 (2007) 2791.
[10] R. Subasri, M. Asha, K. Hembram, G. V. N. Rao, T. N. Rao, Mater. Chem. Phys. 115 (2009) 677.
[11] D. R. Clarke, J. Am. Ceram. Soc. **3** (1999) 485.
[12] T. K. Gupta, J. Am. Ceram. Soc. **7** (1990) 1817.
[13] M. M. Oliveira, Dr. Thesis, Federal University of S. Carlos, SP, Brazil (2002).
[14] L. Hozer, *Semiconductor Ceramics - Grain boundary effects*, 1st Ed., Ellis Horwood (1994) 54.
[15] P. R. Emtage, J. Appl. Phys. **48** (10) (1979) 6833.
[16] J. Lasri, P. D. Ramesh, L. Schächter, J. Am. Ceram. Soc. **83**, 6 (2000) 1465.
[17] M. R. C. Santos, V. C. Sousa, M. M. Oliveira, F. R. Sensato, W. K. Bacelar, E. Longo, E. R. Leite, J. A. Varela, J. Eur. Ceram. Soc. **21** (2001) 161.
[18] M. M. Oliveira, J. H. G. Rangel, V. C. de Sousa, E. R. Leite, P. R. Bueno, J. A. Varela, Cerâmica **52**, 323 (2006) 149.
[19] P. R. Bueno, S. A. Pianaro, E. C. Pereira, J. A. Varela, J. Appl. Phys. **84**, 7 (1998) 3700.
[20] P. R. Bueno, J. A. Varela, E. Longo, J. Eur. Ceram. Soc. **28** (2008) 505.
[21] K. Mukae, K. Tsuda, Y. Nagasawa, J. Appl. Phys. **50**, 6 (1979) 4475.
[22] P. R. Bueno, M. M. Oliveira, W. K. Bacelar Junior, E. R. Leite, E. Longo, J. Appl. Phys. **91,** 9 (2002) 1.
[23] P. R. Bueno, M. R. Santos, E. R. Cassia, E. Leite, E. Longo, J. Appl. Phys. **88**, 11 (2000) 6545.
[24] V. P. B Marques, Dr. Thesis, Institute of Chemistry, UNESP, Araraquara, SP, Brazil (2003).
(Rec. 26/10/2010, Rev. 28/03/2011, Ac. 24/05/2011)